SEVERE THUNDERSTORMS ON 31 MAY 1996: A SATELLITE METEOROLOGY TRAINING CASE

J. Weaver, J. Dostalek, and B. Motta

NOAA/NESDIS/RAMMt
at the Cooperative Institute for Research in the Atmosphere
Colorado State University
Fort Collins, Colorado

J.F.W. Purdom

NOAA/NESDIS/ORA
NOAA Science Center
Camp Springs, Maryland

Abstract

The purpose of this study is to use satellite imagery in conjunction with other meteorological data to analyze several aspects of a severe weather outbreak that occurred over the Central Plains. The emphasis of the paper is on improved analysis techniques that lead to better nowcasts and better short-range forecasts. Topics addressed include the identification and tracking of synoptic-scale systems, nighttime identification of low-level thunderstorm outflow (LTO) boundaries, use of satellite imagery in refining the location of low-level boundaries (such as fronts, drylines, LTO boundaries, etc.), identification of important storm-scale interactions, and many others.

1. Introduction

On 31 May 1996, strong thunderstorms over Kansas and Colorado produced numerous occurrences of severe weather, including large hail, damaging winds and F0 - F2 (Fujita and Pearson, 1976) tornadoes. While the outbreak was not unusual either in intensity or in areal extent, the data set available for studying this case is unique, since several segments of experimental 30-second interval GOES[1] imagery were collected during a tornado outbreak for the first time in history.

The following study utilizes satellite imagery supplemented by other meteorological data to look at several interesting aspects of the 31 May case, including a period during which tornadoes were occurring and 30-second imaging data were being collected. It presents a potpourri of new uses for and new capabilities of GOES data in the nowcast/short-range forecast environment. Results point to the versatility of the so-called "fog/stratus product," new capabilities for looking at storm-scale processes, and analysis of various aspects of storm top behavior. Findings unique to the use of 30-second interval imagery are discussed; they are related to the 15-minute data frequency more commonly available from GOES.

2. Data Sources

Satellite imagery for this study came from both of the GOES vehicles operating at the time. The satellites were designated GOES-8, situated over the equator at 75° west longitude, and GOES-9, positioned over the equator at 135° west longitude. The standard five imaging channels include visible imagery, as well as four infrared channels with central wavelengths at 3.9 μm (a short wavelength, infrared channel used in this research to discriminate water from ice clouds), 6.7 μm (a water vapor channel sensitive to mid- and upper-level water vapor), 10.7 μm (a relatively uncontaminated window channel), and 12.0 μm (a window channel with a slight response to low-level water vapor). For more information on the characteristics and capabilities of these channels refer to Menzel and Purdom (1994).

Other data used in this study include Doppler radar data, standard surface and upper-air observations, and videotape documentation of the tornadic storms. The radar data were from the WSR-88D[2] radars at Dodge City, Kansas, and Pueblo, Colorado. Volume scans of both reflectivity and velocity were available and used in various parts of the study. Videotapes of tornadoes were supplied by observers who were on the scene of the tornadic activity in both Colorado and Kansas (see acknowledgments). These visual observations were vital for resolving critical timing issues between satellite-observed storm features and ground-based outcomes.

3. Some Points of Interest Regarding the Pre-storm Environment

Figure 1 shows standard upper-level charts from 1200 UTC 31 May 1996. The dominant synoptic feature is a low-amplitude long-wave trough covering most of the western United States. A number of short-wave disturbances can be found within the larger flow, but 6.7 μm

[1]GOES — Geostationary Operational Environmental Satellite
[2]WSR-88D – Weather Surveillance Radar, Model 1988, Doppler

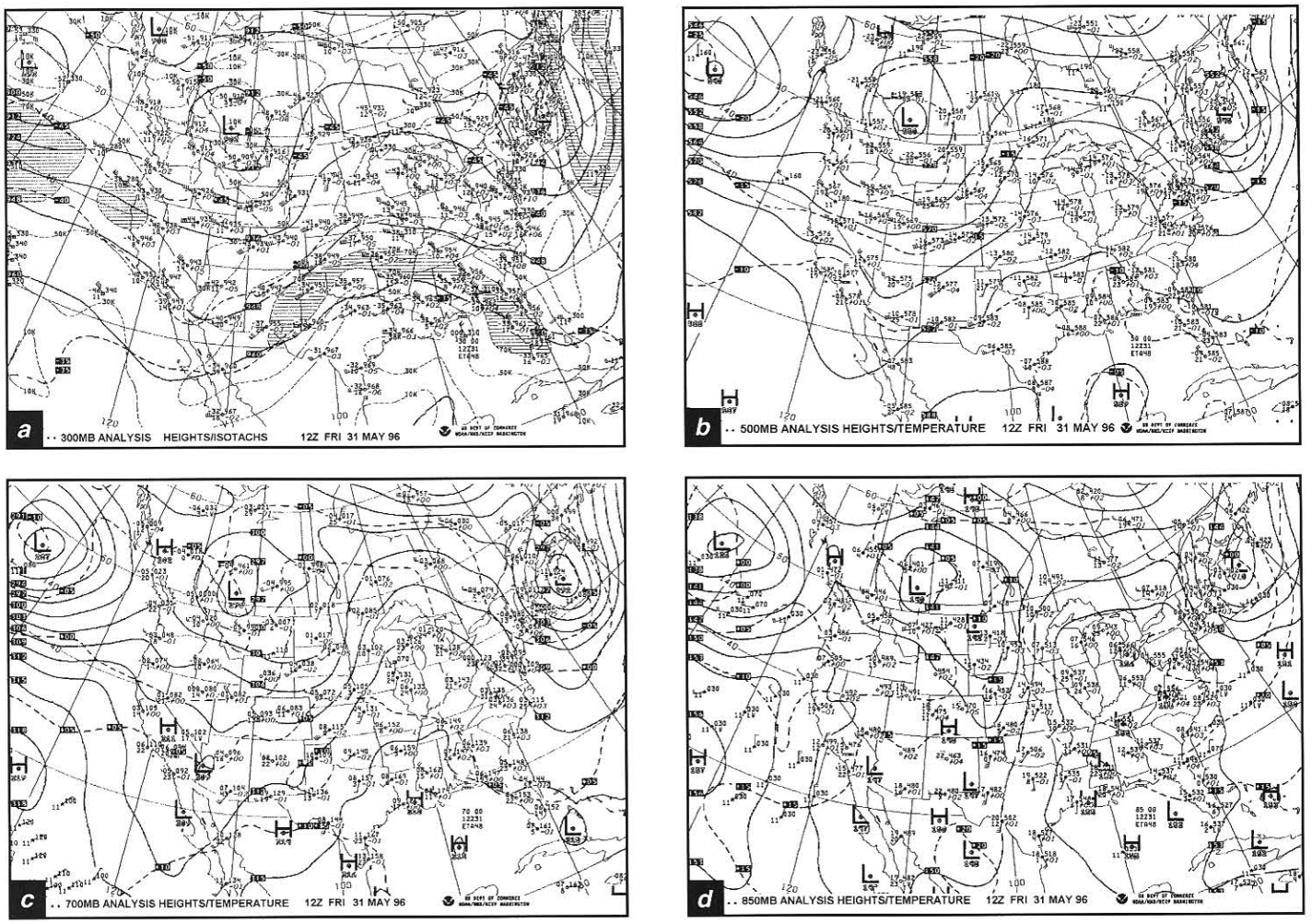

Fig. 1. Standard upper-air charts valid 1200 UTC 31 May 1996. Levels shown are: a) 300 mb, b) 500 mb, c) 700 mb and d) 850 mb.

imagery (Fig. 2a) reveals that the short-wave in northeast Arizona is the most well-defined. A direct comparison between the 6.7 μm image and the morning NOAA/NWS Rapid Update Cycle (RUC) initial analysis finds a relatively good match between the position of the apparent center of the comma-shaped swirl on satellite imagery and the vorticity maximum on the RUC. Some forecasters colloquially refer to the comma-shaped cloud on satellite imagery as the "vort max," implying that the comma cloud seen in the imagery is the same as the 500-mb vorticity maximum found on analyzed upper-air data. However, the comma cloud and vorticity maximum are not the same thing, and precise agreement should not be expected — even when initial model analyses are accurate. The comma cloud on satellite is the result of lifting ahead of, and subsidence behind, an advecting short-wave trough. The analysis of vertical vorticity is composed of directional and speed shears in the wind field. Admittedly, well-organized short-wave troughs usually have a closed center of positive vertical vorticity associated with them, and the closed vorticity contours from model forecasts can frequently be used for predicting the position of these features later in the day. Figure 2b illustrates the point. The figure shows the 1800 UTC, 6.7 μm image with the 6-h RUC forecast of 500-mb heights and vorticity (also valid at 1800 UTC) superimposed. The three nearly parallel lines in Colorado are the extrapolated 6-h positions of the features denoted by "+" signs in Colorado in Fig. 2a. The extrapolation was based on sequential imagery from 1100 UTC through 1400 UTC. These features are colder cloud elements that formed on the 'nose' of the comma cloud - probably in the region of strongest 500-mb positive vorticity advection (PVA) early in the morning. Notice that the extrapolated positions are in extreme northeastern Colorado and one might assume that this is where the extrapolated position of the 'nose' might be. However, notice that the center of the comma swirl in the water vapor image that had been in northern Arizona at 1200 UTC (Fig. 2a), moved almost due east into northwestern New Mexico by 1800 UTC (Fig. 2b). The match between the 500-mb vorticity center, and the center of the swirl is very close at both times. Also note that the area of implied maximum PVA (NE of the vorticity center) associated with the moisture swirl is approaching southeastern Colorado and southwestern Kansas where severe convection did develop later in the day. The colder cloud elements whose extrapolated positions ended up in northeastern Colorado most likely advected with the higher-level flow and away from the leading edge of the water vapor comma swirl.

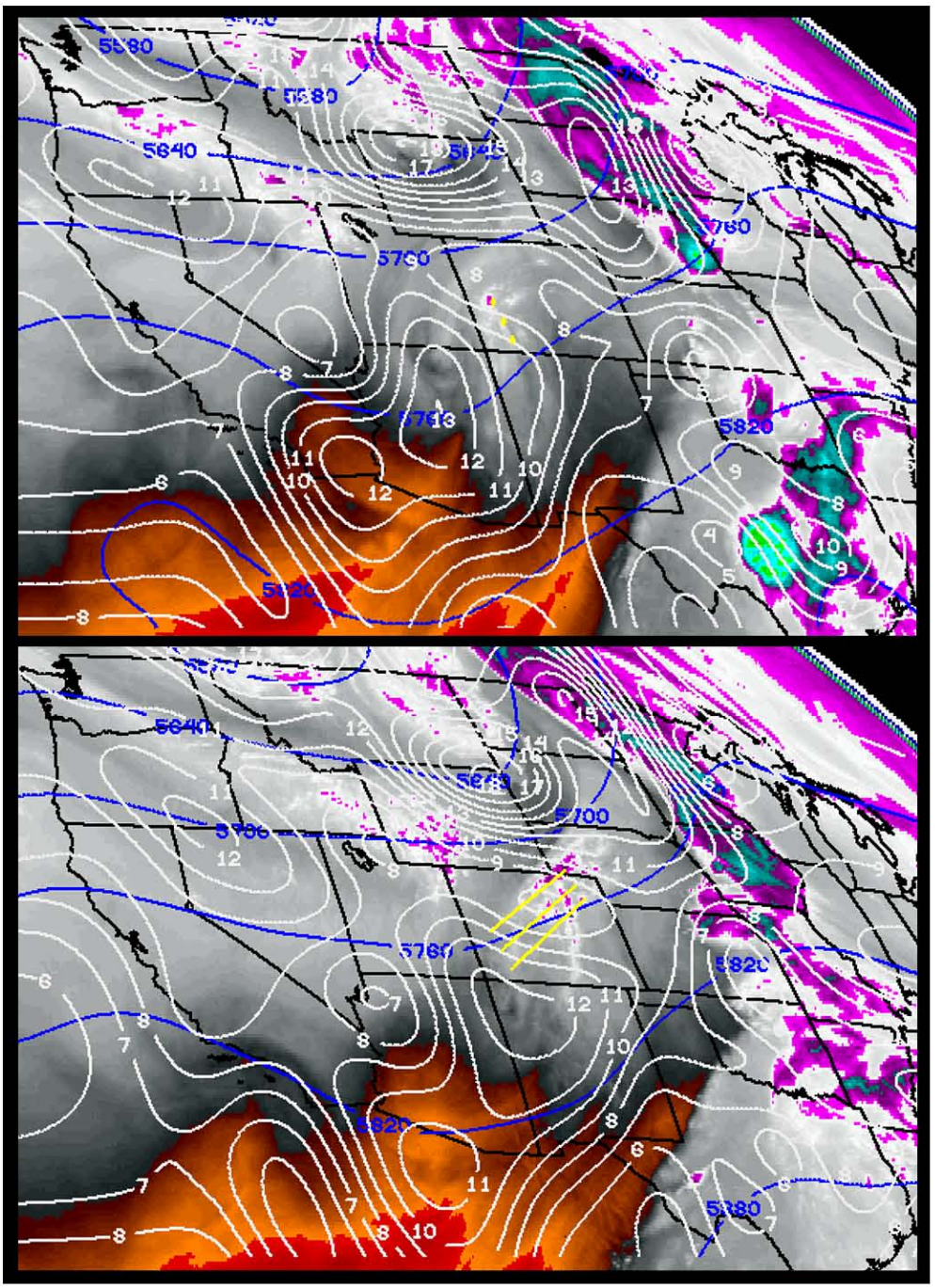

Fig. 2. a) 6.7 μm satellite image taken by GOES-9 at 1200 UTC 31 May 1996. Overlaid is the absolute vorticity analysis at 500 mb from the RUC model. Crosses in southwest Colorado represent the position of three cloud elements that are traceable over the period 1100 UTC through 1400 UTC, and b) 6.7 μm satellite image at 1800 UTC with RUC 6-h forecast 500-mb absolute vorticity. The three dark lines stretching across Colorado are the paths (1400 - 1800 UTC extrapolated) of the three elements highlighted in Fig. 2a.

One of the critical factors in setting up the environment for the 31 May severe activity began the evening before. A low-level jet (LLJ) had formed over the Central Plains, and moisture associated with this phenomenon fueled a line of intense thunderstorms in Nebraska and the Dakotas. Figure 3 shows the RUC surface mixing ratios and winds overlaid on a multi-spectral image product made by subtracting 3.9 μm brightness temperatures from those at 10.7 μm. This difference image (sometimes called the "fog/stratus product") is designed to show water clouds at night (Ellrod 1994; RAMM 1996). In this case, the imagery shows copious stratiform cloudiness associated with the LLJ in central Kansas. In the past, forecasters relied heavily on the REMARKS section of the hourly surface observations. Local remarks reporting stratiform cloudiness at multiple sites were often used to imply abundant low-level moisture for later convective development. With the advent of higher resolution satellite imagery, stratiform regions can be discerned using combined imagery at a 4 km spatial resolution. Many of the important cloud forms that forecasters formerly looked for on the reports from local observing sites can now be seen in the GOES imagery, at a much greater spatial resolution.

Figure 4 shows a series of four 10.7 μm images, and Fig. 5 the fog/stratus product images for the corresponding times and location. An immediate and direct application of this product is its ability to identify regions of stratiform cloudiness associated with low-level thunderstorm outflow (LTO) as described by Dostalek et al. (1997). In these figures, the outflow region is indicated by arrow "A." Arrows "B" and "C" point to small fog or stratus bands associated with lifting along terrain features in Colorado. Notice that the outflow region is much easier to identify in Fig. 5. There is barely a hint of this important feature in Fig. 4. The ability to distinguish water clouds at fifteen-minute intervals is a relatively new capability, made possible by the increased temporal and spatial resolution of the 3.9 μm channel imagery on the new generation of GOES vehicles.

4. Morning Evolution

By mid-morning the situation in the boundary layer had become quite complex. There were several features of particular interest to the forecast problem in Colorado and Kansas. These included a surface low, a warm front, the east-west LTO boundary discussed above, and a dry-

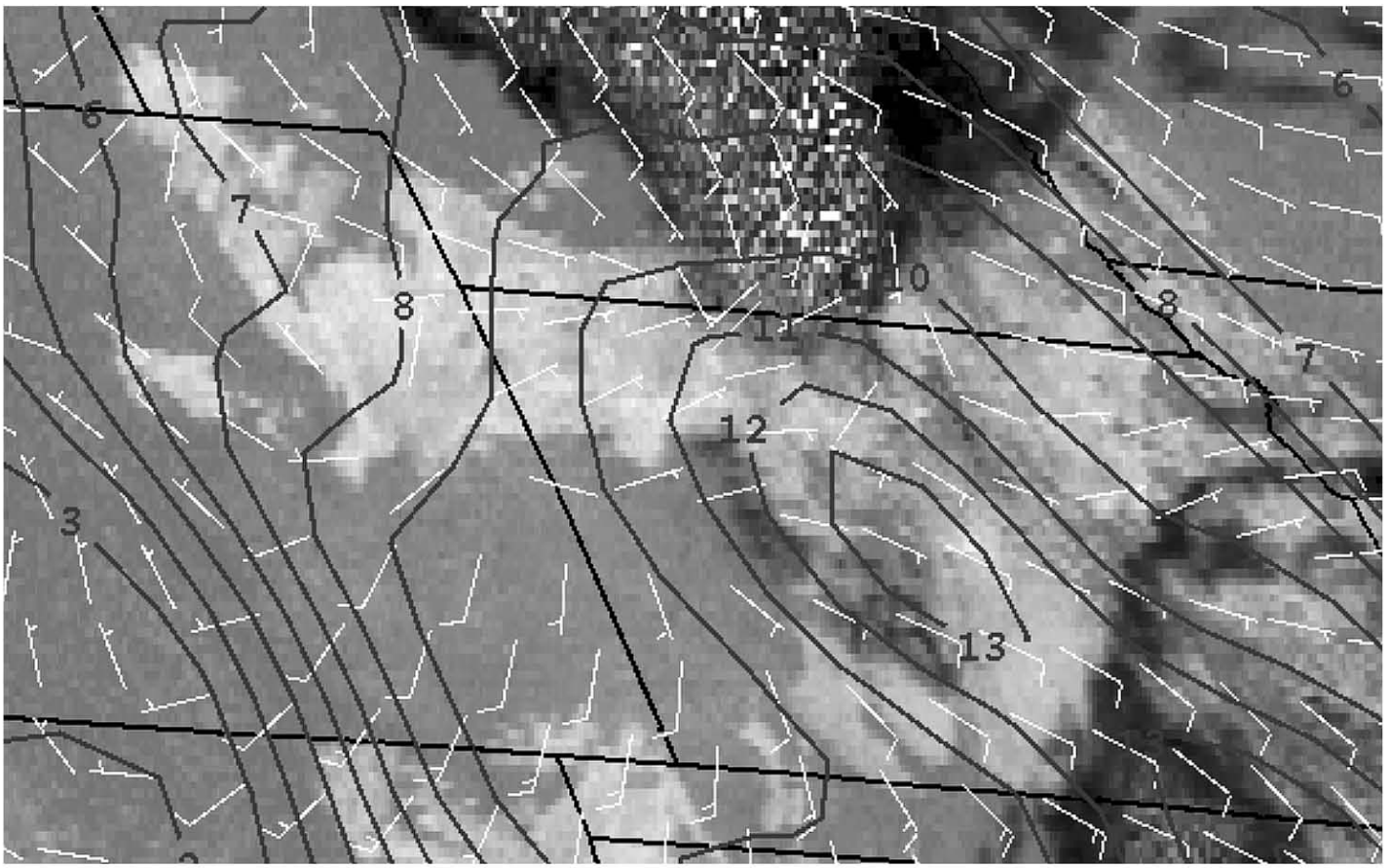

Fig. 3. GOES-9, multi-spectral image product (10.7 μm minus 3.9 μm) at 1000 UTC 31 May 1996 with surface mixing ratio (g kg^{-1}) analysis and surface wind barbs (kt) superimposed. Light gray features are liquid water clouds, darker gray represents cloud-free regions, and the large, speckled features over central Nebraska are cold thunderstorm tops. Figure illustrates low-level moist tongue and southerly flow into central Kansas. Surface wind barbs show convergence along the LTO boundary in northwest Kansas and northeast Colorado.

line. A fifth feature (also not analyzed on standard charts) will also be discussed. This was a weak, north-south oriented low-level mesoscale outflow boundary that was somewhat difficult to identify. It played a significant role in convective development later in the day.

The low pressure system was well-defined and easy to follow. Its position, based on surface pressure and wind observations from National Weather Service (NWS) surface reporting sites, remained relatively constant. The analyzed position matches a circulation center observed on satellite imagery in the cumulus and stratocumulus cloud fields along the southeastern Colorado border. Figure 6 shows a visible satellite image taken at 1615 UTC. Standard NWS surface observations are overlaid, along with a few wind barbs derived from cloud drift wind calculations. The wind barbs match what is qualitatively observed when the imagery is animated. This circulation center was easy to identify on satellite loops throughout the early morning hours, at least until the stratus field dissipated between 1530 and 1615 UTC.

The most difficult of the low-level features to analyze was the surface warm front. Consider the NMC[3] surface analyses for 0900, 1200, and 1500 UTC (Fig. 7), paying particular attention to the location of the warm front. At 0900 UTC, the analysis shows the front extending southeastward from the low in Colorado, through southwest Kansas and central Oklahoma. By 1200 UTC, the front (now stationary) had apparently jumped into extreme southwest Oklahoma. Surface observations seem to confirm this position with cooler temperatures to the north and east of the boundary. However, pre-dawn infrared satellite imagery clearly shows the reason for this apparent drastic jump southward. There were numerous thunderstorms occurring in southwest Oklahoma associated with the trailing edge of the short-wave which had helped to trigger the convection in Nebraska and South Dakota. The warm front at 1200 UTC was probably in southern Kansas, and the analysis should have looked more like that shown in Fig. 8. By 1500 UTC, this elusive boundary seems to have jumped again, this time some 250 miles north to a position in extreme northern Kansas. Here, the analyzed position was probably closer to the actual, though perhaps a bit too far north. Figure 9 shows a visible wavelength image from 1531 UTC. Notice cloudiness in northwestern Kansas. That was the region where stratiform clouds had formed above the overnight outflow. It is clear that the (now) stationary front did not push north of this location at the surface, and we suggest the analysis in Fig. 9 is a better "fit" to describe what had actually taken place.

[3]NMC — The National Meteorological Center, now called the National Centers for Environmental Prediction, NCEP.

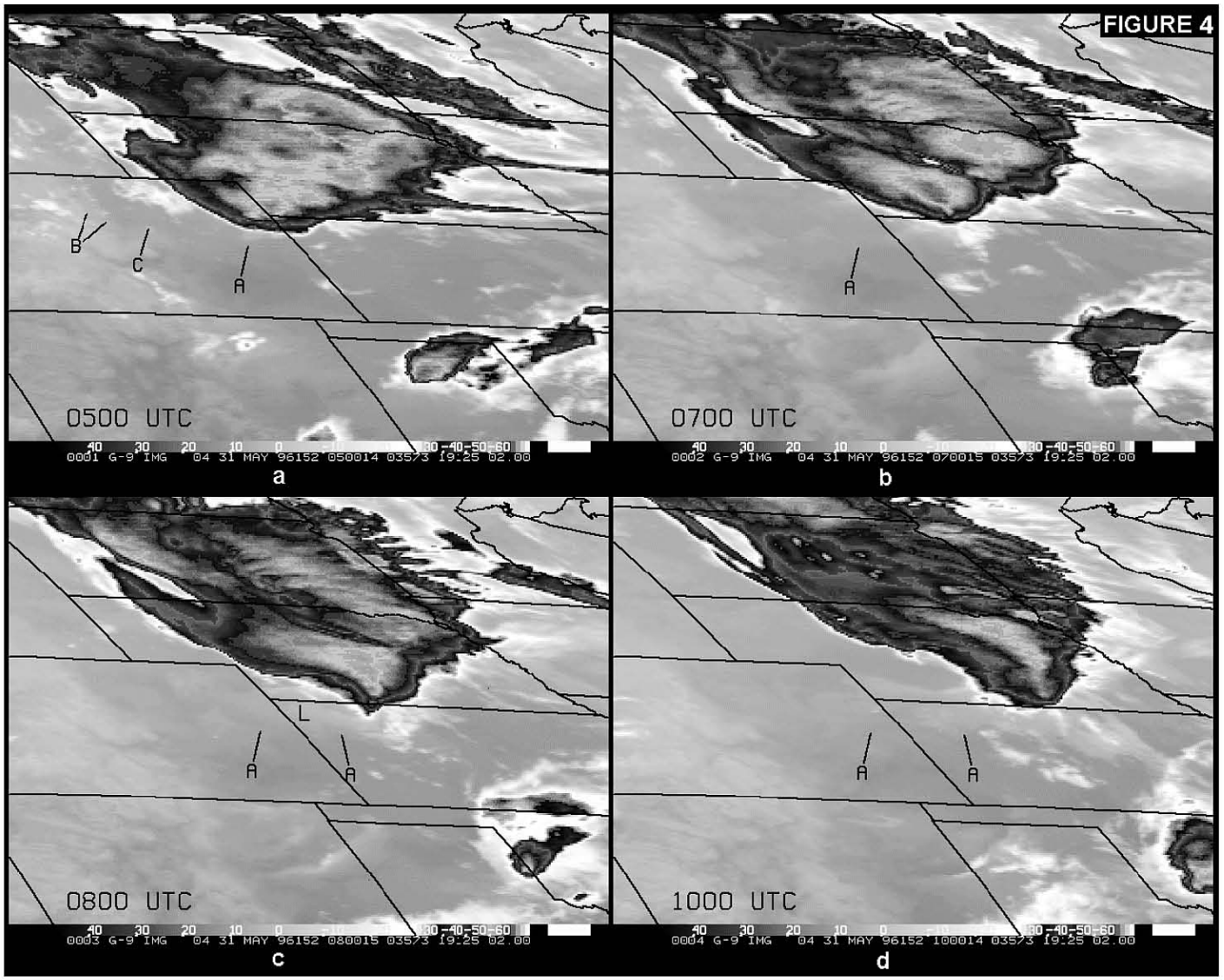

Fig. 4. GOES-9, 10.7 μm satellite imagery from 0500 - 1000 UTC 31 May 1996 focusing on a line of thunderstorms moving through Nebraska and South Dakota. The southern end of the complex is at the Colorado - Nebraska - Kansas border at 0500 UTC. The leading edge of the low-level thunderstorm outflow air (indicated with letter "A") is not evident in these images due to a lack of thermal contrast between clouds that have formed along the boundary and the cool ground. Brightness temperatures along gray bars are in degrees C.

The last NMC-analyzed surface feature of interest was a dryline, which stretched southwestward from the low in southeastern Colorado. As in the case of the surface low, we feel that the NMC sea-level pressure chart did a good job of defining the dryline's location. In this case, the boundary was oriented parallel to the mean winds (from the surface to about 500 mb). It showed no signs of eastward movement throughout the morning hours, and should not have been expected to move very far eastward as long as the mixed flow vector had no orthogonal component. Actually, a slight eastward propagation did occur later in the afternoon, but that movement resulted solely through the mechanism of diurnal mixing of the low-level inversion (e.g., Schaefer 1973).

Finally, a few words about another important feature that was not analyzed on the standard analysis charts. A careful perusal of late morning, visible satellite imagery (Fig. 10) finds a subtle difference in the appearance of the cloud fields in eastern Kansas and Oklahoma versus those in western portions of the same two states. The western "airmass" has an undisturbed appearance that reveals itself as numerous, regularly-spaced cumulus cloud streets. The large region to the east is a chaotic mixture of various cloud types at a number of levels. This is because the eastern area was subjected to round-after-round of thunderstorms over several hours prior to the time of this image. It will be shown later that the point where the boundary separating these two regions met the LTO boundary/stationary front was where the first severe storm in Kansas developed.

5. Storm-scale Features of Interest

A new round of convection began in east-central Colorado at roughly 1730 UTC. This new development coincided with the arrival of the short-wave trough from

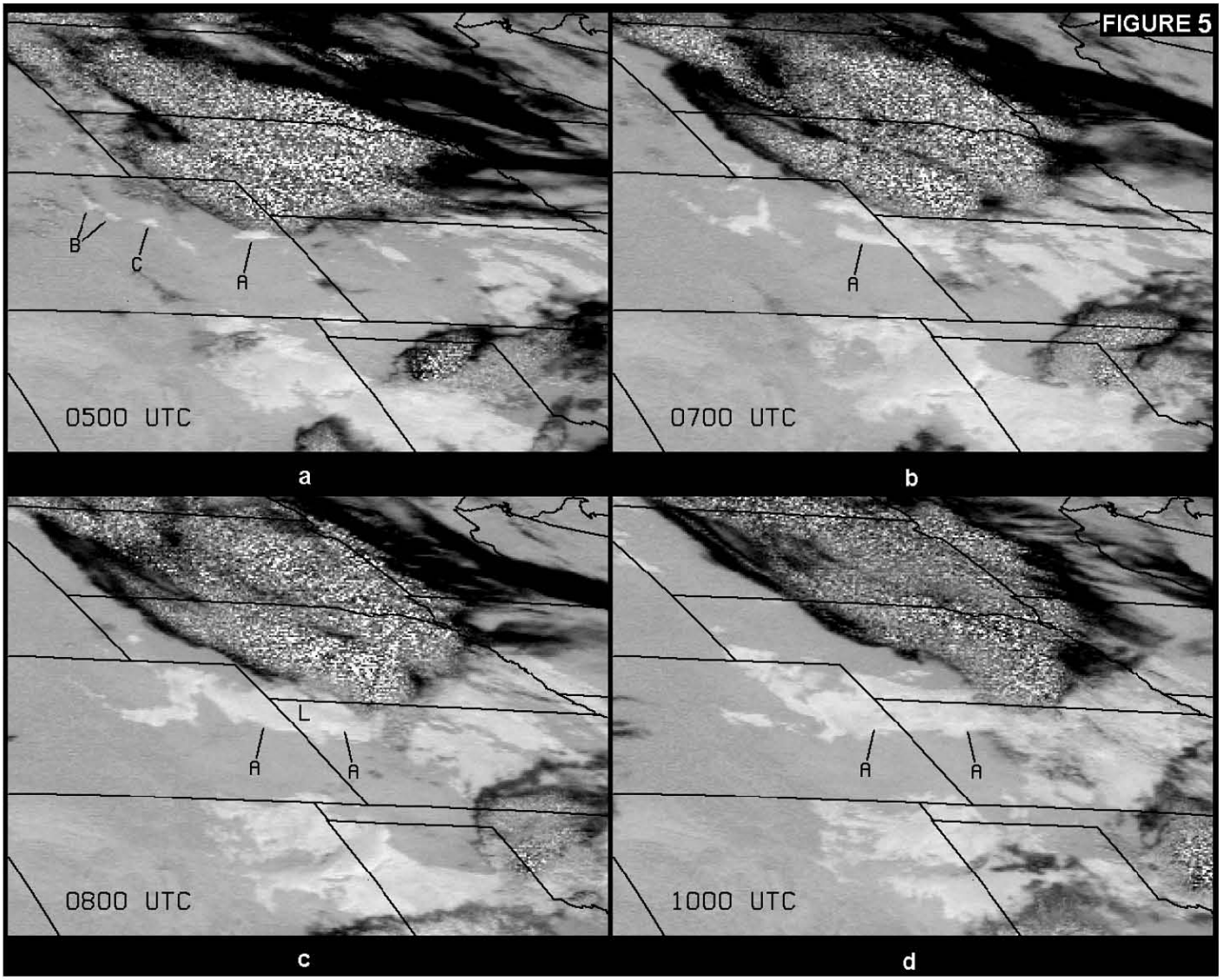

Fig. 5. Same as Fig. 4, except imagery shown is the 10.7 μm minus 3.9 μm, multi-spectral image product (sometimes called the "fog/stratus product"). This product is designed to differentiate liquid water clouds (light gray) from ice clouds at night. Notice how clearly the stratiform clouds along the outflow boundary show up. Also, note that the stratiform layer above the outflow ("L" in the figure) fills in with time.

Arizona. The storms formed along an elevated terrain feature known as the Palmer Lake Divide, and moved off toward the east-southeast. The activity quickly expanded into a short squall line segment. These storms would produce a family of small tornadoes in southeast Colorado beginning around 2330 UTC (Fig. 11). At about the same time the Palmer Lake Divide convection was beginning, thunderstorms formed along the dryline in southeast Colorado and the Oklahoma panhandle. Those storms also became tornadic. A third convective region was triggered where the LTO boundary/stationary front intersected the north-south boundary discussed above. This activity first appeared at about 1915 UTC and quickly became severe, producing large hail in central Kansas within 45 minutes of its first appearance. Finally, several storms formed between 2000 and 2100 UTC along the remnants of the east-west LTO boundary in west-central Kansas. Each of these four convective regions will be described and discussed separately.

a. The Palmer Lake Divide-generated storms in Colorado

As noted above, the convection which began at 1730 UTC on the eastern end of the Palmer Lake Divide moved off almost immediately toward the southeast. Traveling as it did across mostly open country, it is difficult to know what occurred before 2220 UTC, but as the activity approached the town of Eads, Colorado, several reports of severe weather were received (NOAA 1996). Between 2220 and 2245 UTC there were reports of hail up to 2 inches in diameter, along with a report of wind gusts up to 70 mph (measured at 2240 UTC). The severe wind gust report corresponded to the sudden appearance on visible imagery of a twelve-mile-wide wedge of low-level stratocumulus cloudiness which rushed out at about that same speed from the southeastern edge of what had become a squall line (Fig. 12). The event occurred during a 30-second interval imaging

sequence, and was quite easy to follow as it made its appearance over an interval of about 1 1/2 minutes. Such rapid mesoscale evolutions are impossible to document using radar or satellite data in normal scanning modes. When we look at 15-minute interval satellite data alone, the event is much more difficult to track. Ten out of twelve meteorologists surveyed informally at CIRA did not notice the feature when presented with 15-minute data alone. It was detected by most volunteers on 7-minute interval data, but became obvious to all participants at a 3-minute interval or less sequence. The implication is that certain small, but potentially important, thunderstorm-scale features may not be detectable at the standard data collection interval of 15-minutes. Of course, if detection of such features is to be relevant, the data must be made available to the forecaster in a timely manner.

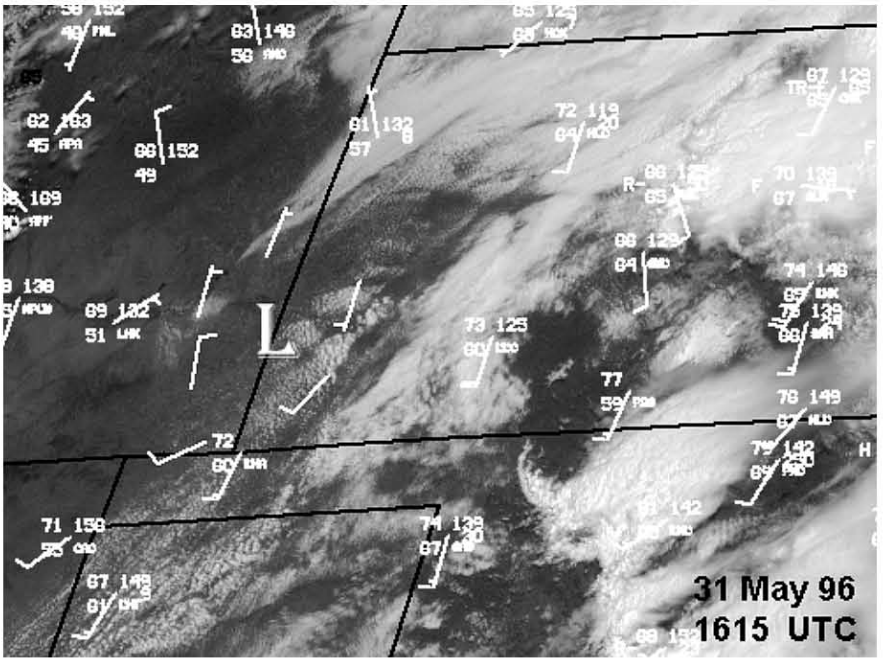

Fig. 6. GOES-8 visible image at 1615 UTC 31 May 1996. The approximate position of the surface low is shown. Standard hourly surface observations are plotted, along with a few cloud-track winds in the vicinity of the low. The combined wind field illustrates the circulation around the system.

The thunderstorm outflow, represented by this small wedge of low-level cloudiness, seemed to play a continuing role in the events over about the next half hour in the form of an apparent interaction with a storm to its southwest. On animated satellite imagery the western edge of the outflow feature can be followed as it moves southwestward toward the southern end of the squall line. A merger can be seen taking place between 2311 and 2315 UTC. This event was followed almost immediately by the development of a 1/4-mile-wide tornado which produced F1 damage to grain bins, a barn, and a mobile home. The mechanism of sudden tornado development is unknown, but the evolution bears a striking similarity to other such occurrences (e.g., Weaver and Purdom 1995, or Browning et al. 1997). All of the event locations and times were well documented by in-situ storm observers (see acknowledgments).

We should also note here an interesting way of using the GOES imagery for identifying subsidence

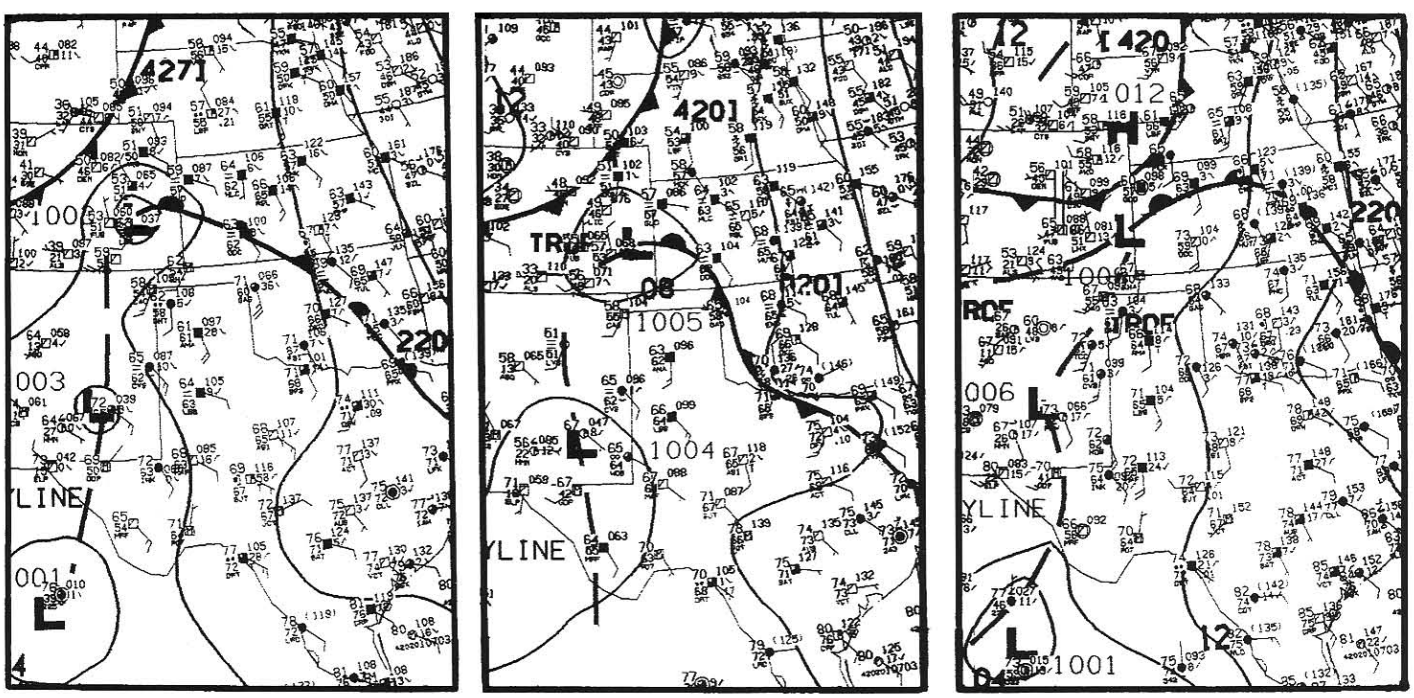

Fig. 7. Standard NMC surface analyses from 31 May 1996. Times shown are: a) 0900 UTC, b) 1200 UTC, and c) 1500 UTC, respectively. Plotting conventions are standard U.S.

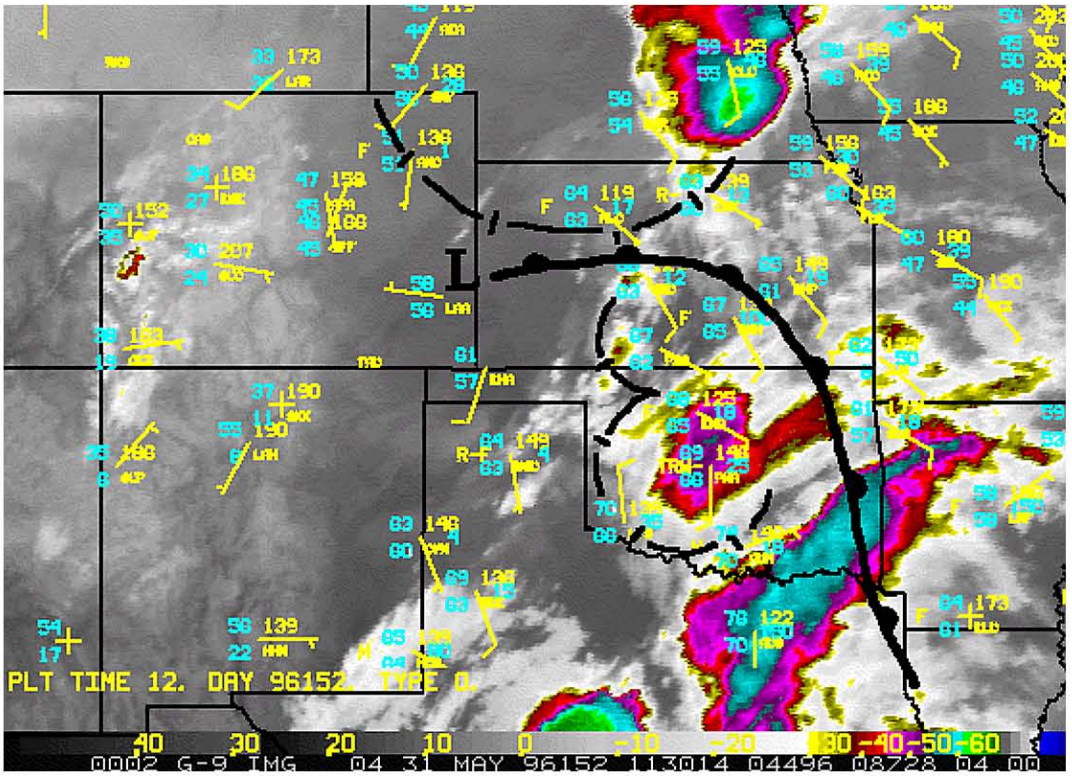

Fig. 8. Re-analysis of the 1200 UTC surface chart using supplemental information from the 1130 UTC 31 May 1996, GOES-9, 10.7 μm imagery remapped to a Mercator projection for ease in comparison.

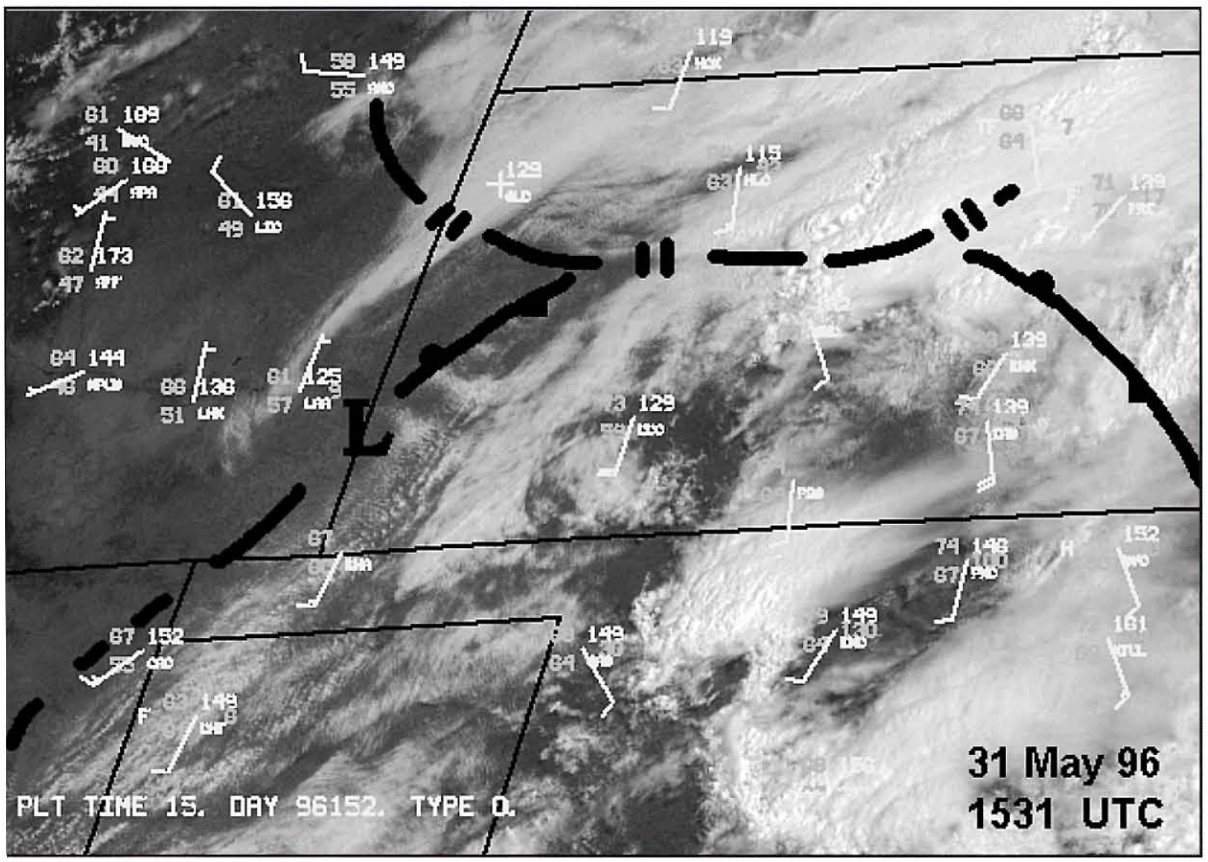

Fig. 9. Re-analysis of the 1500 UTC 31 May 1996 surface data using supplemental information from the 1531 UTC, GOES-8 visible wavelength imagery, along with continuity arguments as described in text.

associated with an LTO boundary, and perhaps even learn a little about the intensity of the storm. Figure 13 shows a series of visible images for the entire region discussed in this paper. Notice the multiple-layered cloud field to the southwest of the Palmer Lake Divide storm complex. In the first image, a small arc cloud line (associated with the storm's LTO boundary) stretches off to the southwest, then curves around to the west. There is a small group of clouds shaped like the number seven just south of the LTO boundary (labeled "mid" in Fig. 13). It is casting a shadow both onto the ground, as well as the clouds composing the boundary. Next, notice the somewhat larger, oval-shaped cloud mass just west of this feature (labeled "upper" in Fig. 13). Careful perusal of the imagery shows it to be casting a shadow onto the "seven." Thus, the image sequence illustrates at least three levels of cloud: 1) a group of low-level clouds associated with the LTO boundary, 2) a mid-level deck, and 3) an upper, oval-shaped cloud patch. Notice in the sequence that as the middle-deck is undercut by the LTO boundary, the mid-level clouds dissipate. This can be seen much more clearly with animated imagery. The cloud top height of this deck was estimated using the GOES-8, 10.7 μm infrared temperature and the DDC evening sounding, and found to be at roughly 18,000 feet AGL. Thus, subsidence associated with the LTO boundary seems to have affected the atmosphere to at least this height. It is not known whether all of the dissipation observed in the mid-level deck can be ascribed to the subsidence above the stable, LTO airmass, but it clearly occurs as the two intersect.

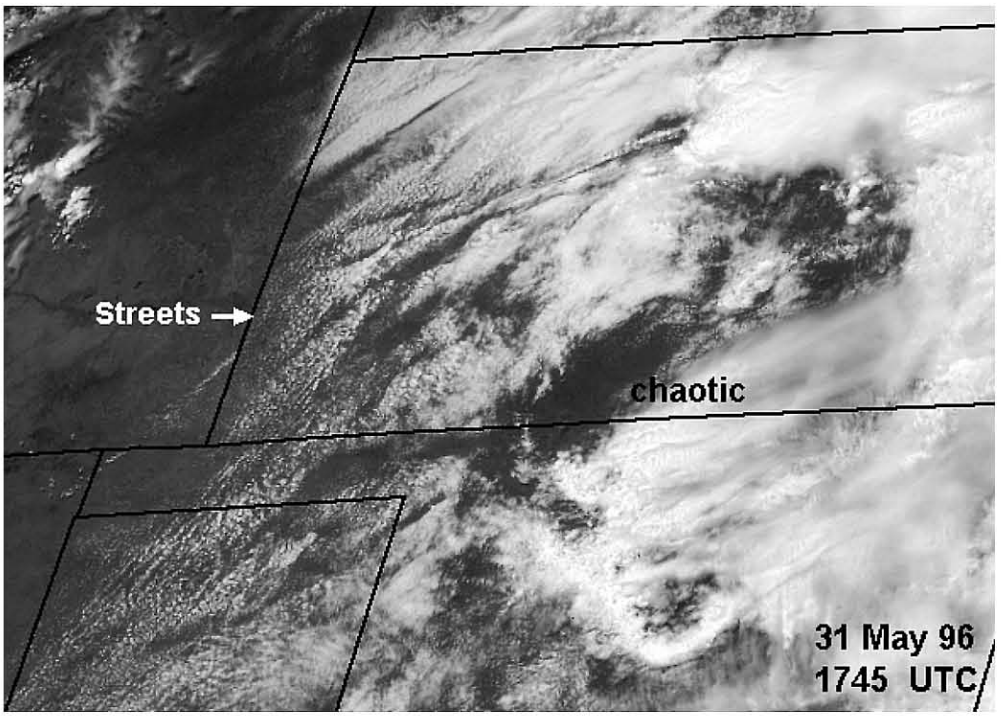

Fig. 10. GOES-8 visible wavelength image from 1745 UTC 31 May 1996, highlighting the different airmasses apparent in western versus eastern Kansas.

The upper cirrus deck was at roughly 32,000 feet AGL. Its source was a thunderstorm which dissipated in south-central Colorado. The remnant anvil could be followed from around 2125 UTC until dark on the visible imagery. In a two-hour long loop, the patch of cirrus could be seen to be eroding slowly, but at a rate that did not change as it crossed over the LTO boundary. Neither the thunderstorm nor the LTO boundary seemed to have any effect on the cirrus feature. The

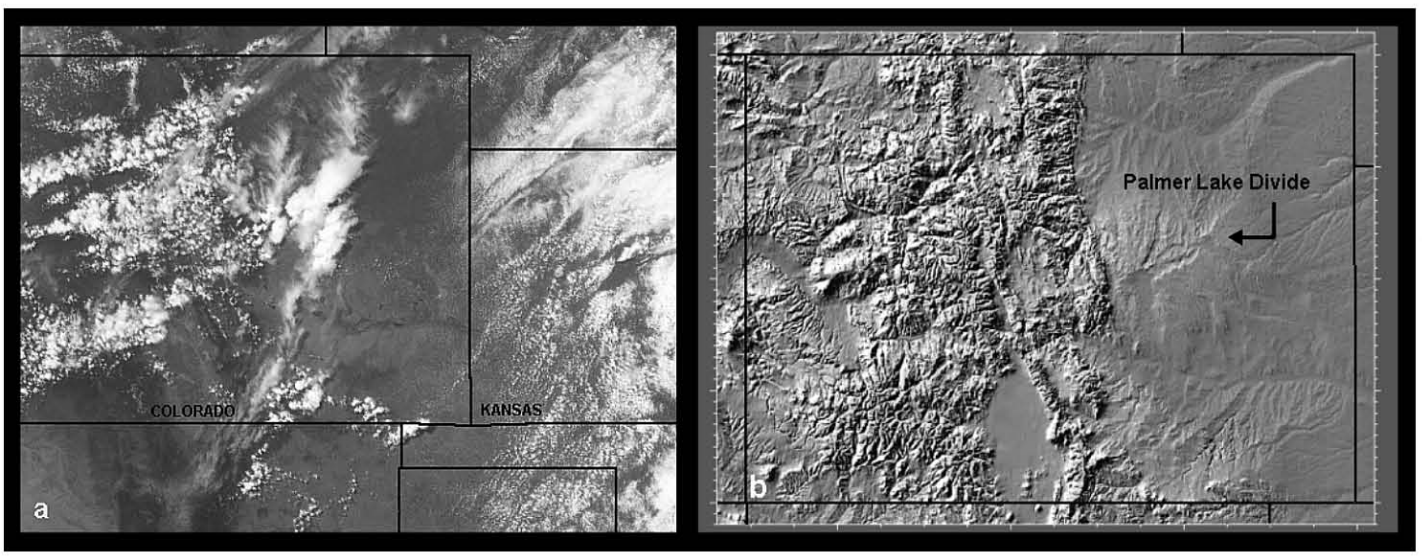

Fig. 11. a) GOES-8 visible image at 1845 UTC 31 May 1996. Image is remapped to Mercator projection for ease in making direct comparison with topography, and b) Colorado topography showing location of Palmer Lake Divide (see text).

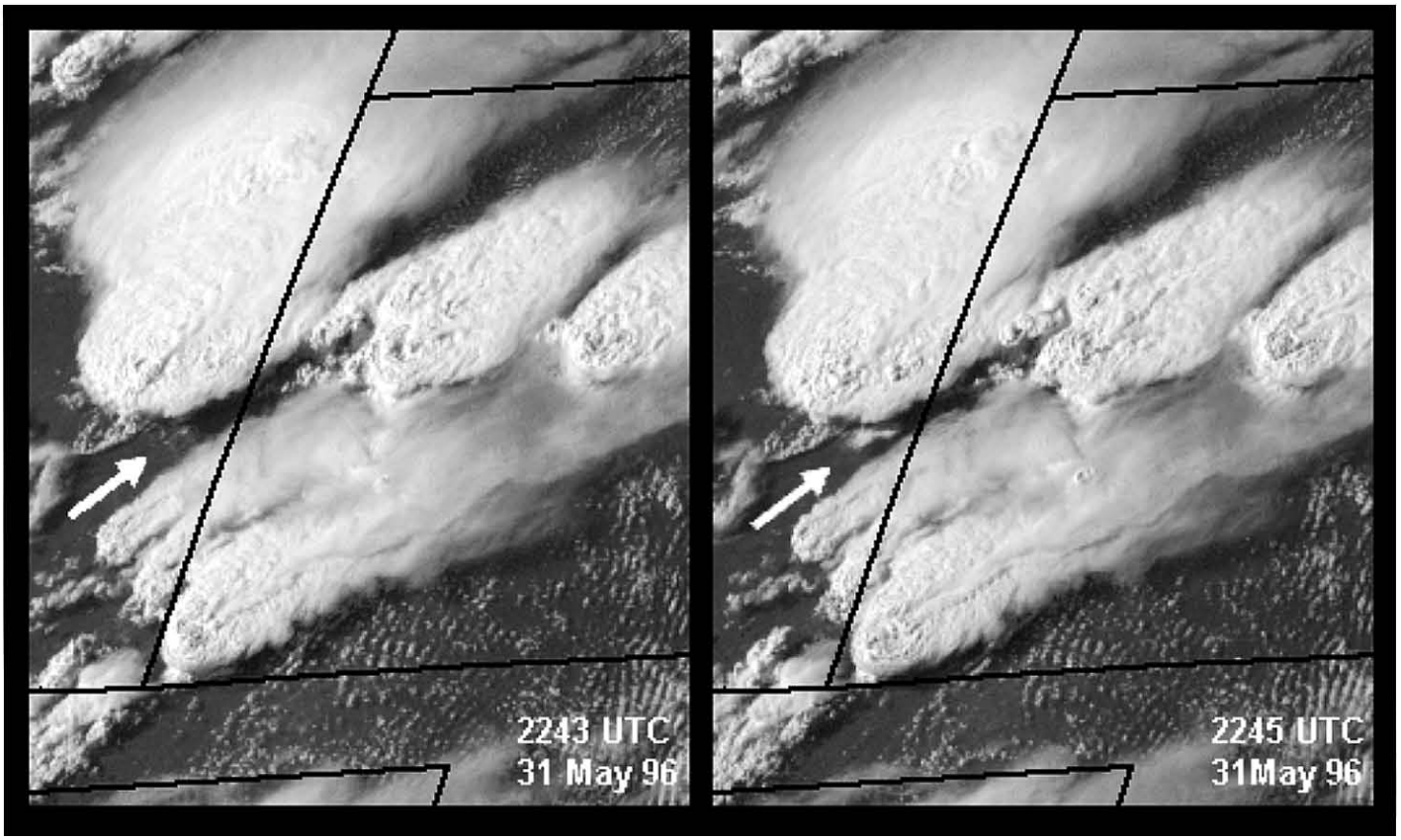

Fig. 12. GOES-8 visible images of extreme eastern Colorado and western Kansas taken on 31 May 1996. The figures show the sudden appearance of a low-level cloud feature just as 70 mph outflow winds were being reported at the surface. Super Rapid Scan imagery were being collected during this period. Times shown are 2243 UTC and 2245 UTC.

failure of the upper deck to respond even as it approached the storm's anvil suggests that the storm was not producing an intense enough updraft to build an anvil level region of high pressure and subsidence. Indeed, perusal of the 6.7 μm imagery around this time and later (not shown), finds no indication of subsidence around this storm's anvil. It is not surprising that the tornadoes associated with this activity were short-lived, rope-like and weak.

b. Dryline storms

The dryline activity formed in the extreme northwestern tip of the Oklahoma panhandle (Fig. 11), then moved quickly into southeast Colorado. By 2025 UTC, it had begun to produce severe weather in the form of large hail and funnel clouds. However, it wasn't until it had moved into the southwestern tip of Kansas (Fig. 12), that the first tornadoes were reported (at 2252 UTC). As with the Palmer Lake Divide storm, the tornadoes produced by this activity were small and relatively weak (F0, NOAA 1996) — although an assessment based strictly on damage has little meaning out on the open prairie.

One of the more interesting features of this storm (as well as with the so-called "Ness City" storm to be discussed below) was an apparent cyclonic rotation in the overshooting top (OST) region of the thunderstorm anvil on visible satellite imagery. This "rotation" began at roughly 2300 UTC, and continued until just after sunset, when the visible imagery became unusable. The apparent rotation at anvil-level seems particularly significant in this case, because the WSR-88D data from Dodge City (not shown) indicated a mesocyclone at low- and mid-levels of the storm throughout this time period. Nearer to storm-top, the radar also showed cyclonic shear, though weaker and less organized. One is tempted to make what seems to be the "next logical step;" i.e., associating the in-storm circulation with the apparent rotation seen in the anvil-level cloud elements. However, analysis of cloud-motion trajectories computed using 1-minute and 30-second interval imagery reveals that anvil rotation was probably not taking place.

Figure 14 shows storm-relative trajectories (assuming a storm motion from 263° at 6 ms^{-1}) computed for various anvil-level cloud elements superimposed on the 2309 UTC visible image. When actual cloud elements are tracked in this manner, it is clear that the apparent cyclonic circulation is simply the result of cloud elements diverging around the OST, as well as complexities of motion induced by there being two separate overshooting tops in the vicinity of one another. Further complications result because the cloud elements on the northeast side of the OST were obscured by cirrus. Occasional glimpses through the cirrus, and brightness changes in the cirrus field itself, may also contribute to the overall perception of rotation.

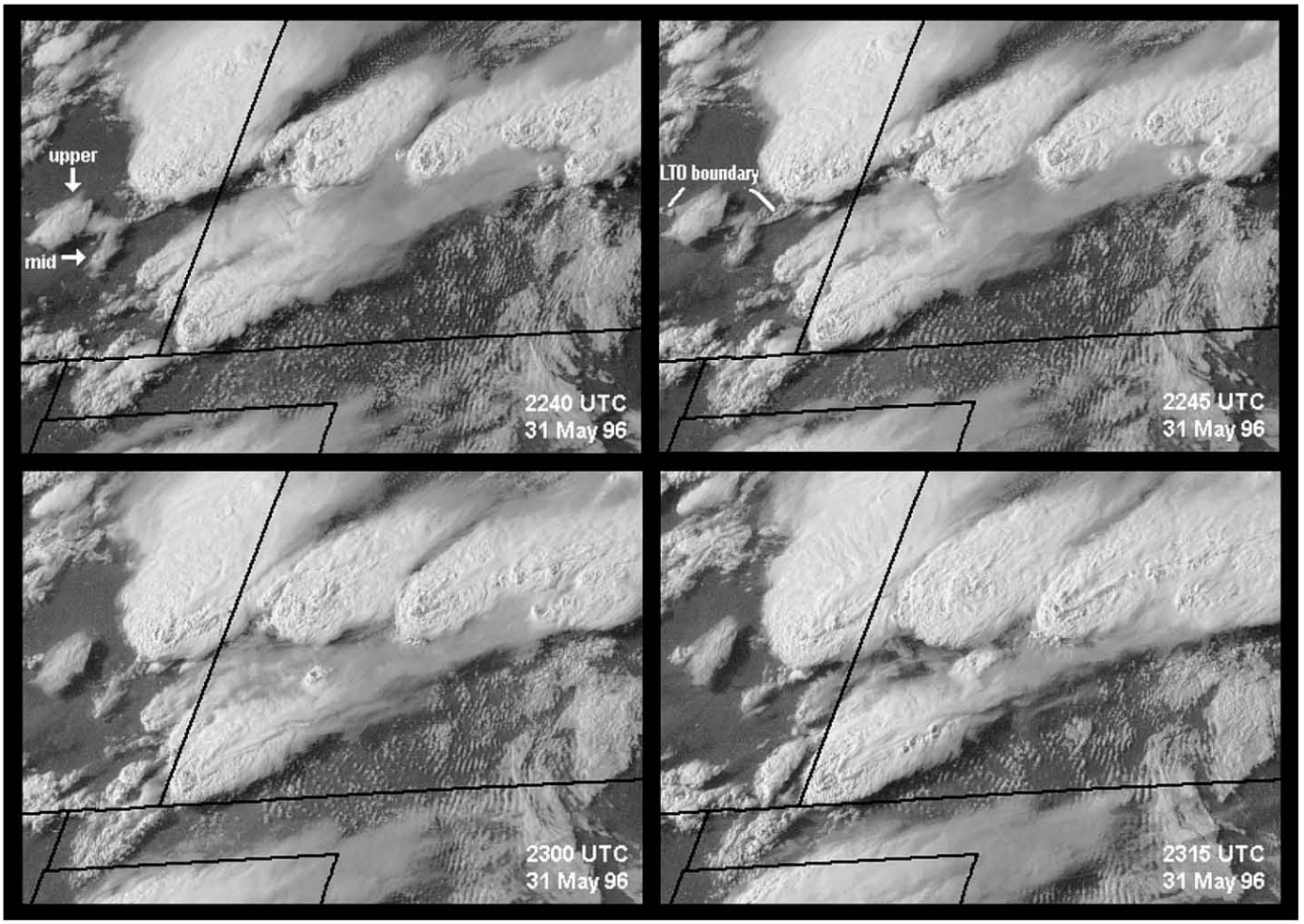

Fig. 13. GOES-8 visible imagery from 31 May 1996. Times as labeled. Sequence illustrates the dissipation of mid-level cloudiness as it moves across an LTO boundary in southeast Colorado. Note that the higher cloud mass does not dissipate.

The preceding point is an important one to remember anytime one is viewing data in motion. The perception and interpretation of motion by an observer can frequently be incorrect. Many times a person will fit pattern-to-motion in an attempt to facilitate the understanding of a situation. In fact, it has long been known that elements in a given environment that seem to move together systematically tend to become perceptually grouped by a human observer (Wertheimer 1937). Cutting and Proffitt (1981) argued that "object-relative" versus "observer-relative" motions have vastly different perceptual significances. Observer-relative motion tends to specify where an object is, and how it is moving, while object-relative (in this case, storm-relative) motion tends to specify what an object is. Thus, by constructing a storm-relative loop, we are attempting to better understand the nature of the object — in this case what appears to be a rotating storm top.

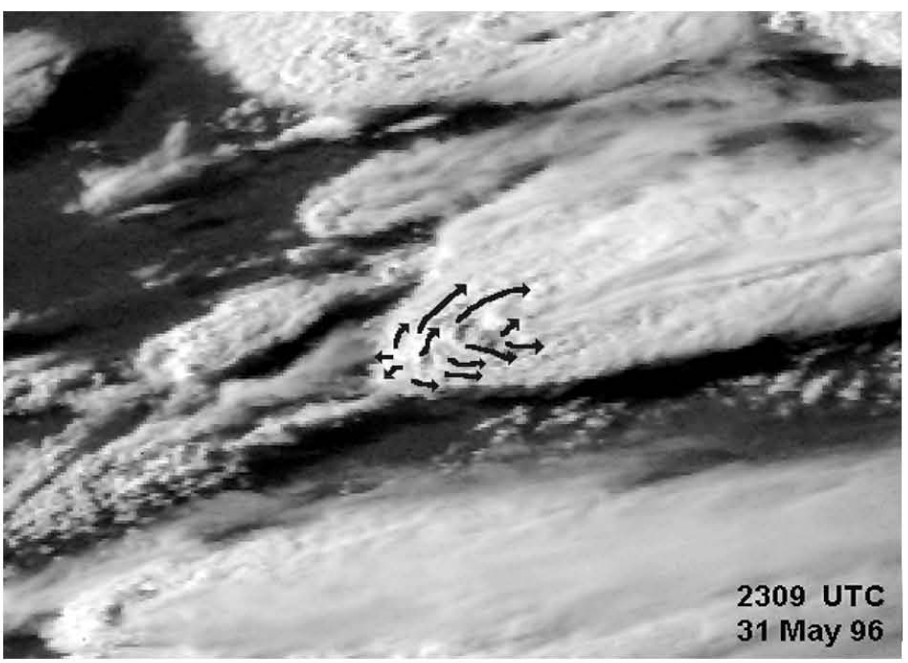

Fig. 14. Visible satellite image at 2309 UTC 31 May 1996 with storm-relative trajectories of several cloud elements superimposed. Sorm motion vector was from 263° at 6 ms^{-1}. Time period over which the trajectories were calculated was from 2255 UTC through 2339 UTC.

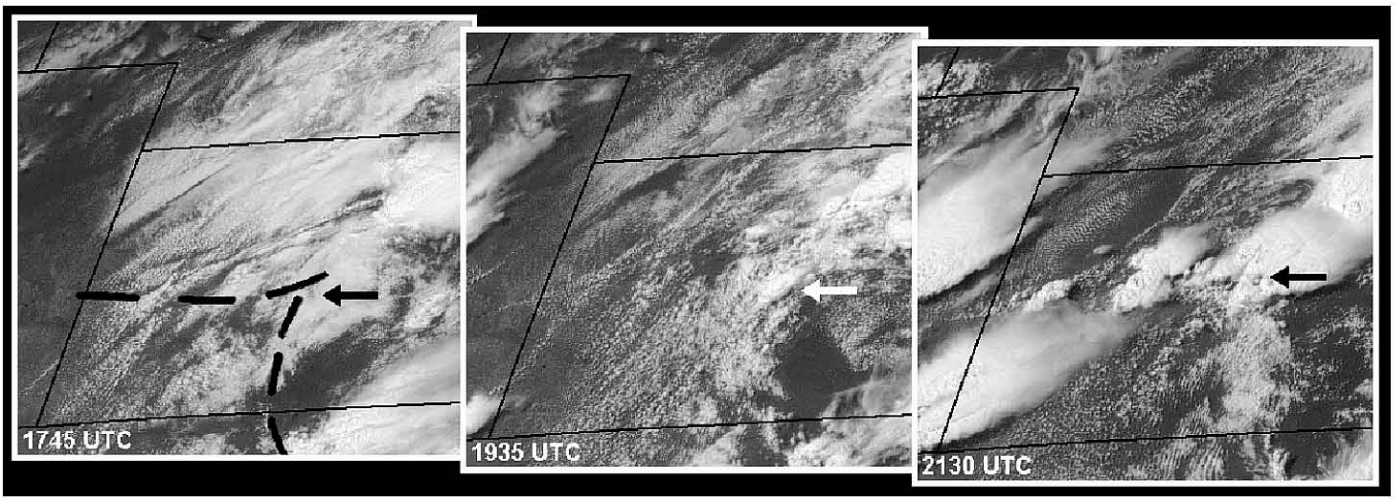

Fig. 15. Time series of GOES-8 visible images from 31 May 1996. Times as labeled. The sequence illustrates the development of severe thunderstorms at the intersection of the LTO boundary, which formed due to an MCS in Nebraska and South Dakota, and a larger north-south LTO boundary in south central Kansas.

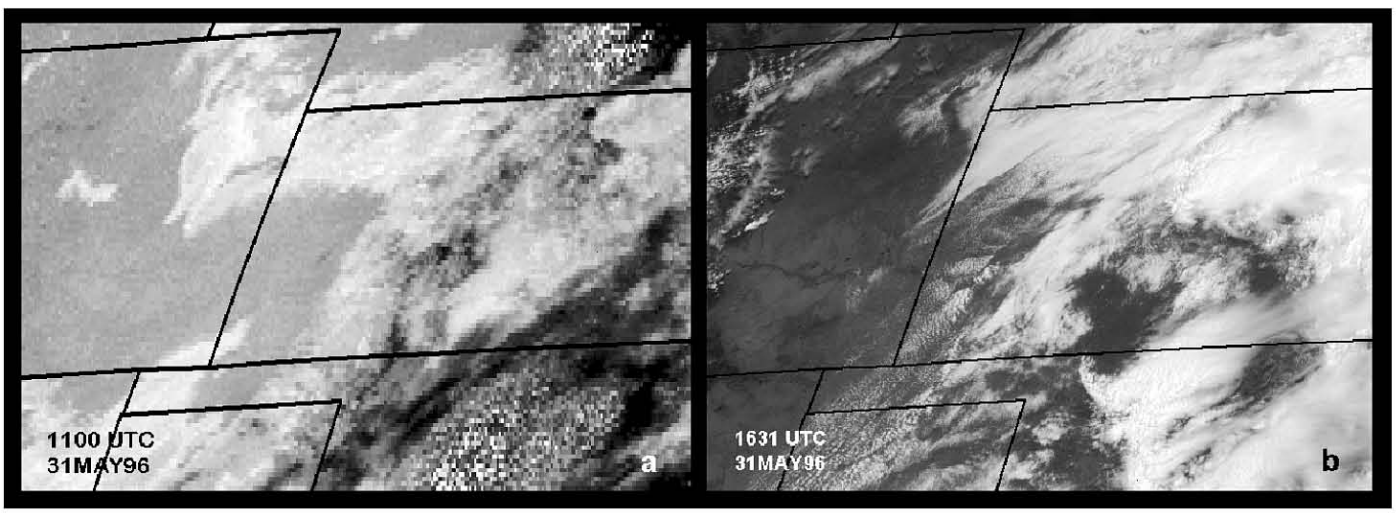

Fig. 16. a) GOES-9 fog/stratus product image (made by subtracting 3.9 μm values from those at 10.7 μm) remapped to a GOES-8 projection valid 1100 UTC 31 May 1996; b) GOES-8 visible image taken at 1631 UTC 31 May 1996. Light-colored cloud pattern near the top center on the fog/stratus product image marks stratiform cloudiness associated with an overnight LTO boundary. Compare a) with b) the visible image taken 5 1/2 hours later.

Cutting and Proffitt (1982) also found that the human visual observation/interpretation system tends to minimize relative motions. When viewing a set of motions as a singular system, humans tend to interpret relative shears as closed circulations. Thus, careful measurement is important when trying to interpret such features on sequential imagery. In this case, the 1-minute and 30-second interval imagery allowed us to properly interpret the motion at storm top as divergence and speed shear.

c. Storms at the intersection of the two LTO boundaries

Figure 15 shows a series of visible satellite images during the period when activity in this region was first forming. The intersection was extremely important to residents of Barton, Ellsworth, Rice, and Saline counties in Kansas, since deep convection continued to regenerate in the area during the entire afternoon and evening, and was severe for most of that period. A report of 1.0 in. diameter hail at 2007 UTC was the first in a series of more than two dozen reports of hailstones up to 2.75 inches. Hail and torrential rains continued over the same four-county area for more than eight hours, and culminated in flash floods that brought one-to-two feet deep water to many locations. Satellite imagery was extremely useful in showing not only the continuous regeneration of large storms, but also the reason for the regeneration. By identifying the reason for the apparently anomalous behavior, the forecaster can more easily make decisions concerning the probability of its continuance, and the issuance of warnings or advisories.

d. Western Kansas LTO boundary convection

The activity along the east-west LTO boundary was the last to develop. It produced the strongest torna-

does, with the maximum intensity reported at F2. The boundary itself was difficult to track after mid-morning, since the stratiform cloudiness began to dissipate early. During the early morning hours, the boundary could be identified on visible data as an overcast region to the north versus mostly clear skies to the south of its position (e.g., Figs. 5 and 6). However, the difference probably would not have been attributed to an LTO boundary if one were not aware of its existence in advance. Compare Fig. 16a and 16b. The stratiform clouds revealed by the fog/stratus product at 1100 UTC can be tracked through mid-morning on the visible imagery. Shortly after 1631 UTC the stratus deck began to dissipate, but one is tempted to speculate that there was a residual cool, moist layer where the stratiform clouds had been. Imagery created from GOES sounder data provides additional evidence for such a moist layer, though it was not available in real time. Figure 17 shows an image made from the GOES-8, channel 10 sounder data after most of the stratiform cloudiness had dissipated. This channel responds to water vapor in the 850 to 500 mb layer, peaking around 675 mb. Notice that the area north of the LTO boundary location shows up slightly brighter (cooler in this lookup table) than the area to its south. This cool layer is detectable through at least 1946 UTC, which is about the time that the east-west line of thunderstorms began to develop. By carefully comparing Fig. 17 with the visible image at the same time (Fig. 10), it is evident that the channel is not responding much, if any, to the underlying cloud field. The sounder imagery clearly shows that the outflow was still having an effect on the mesoscale atmosphere long after the obvious signs had disappeared. Figure 15 shows the developing east-west line of thunderstorms along the LTO boundary at 2130 UTC.

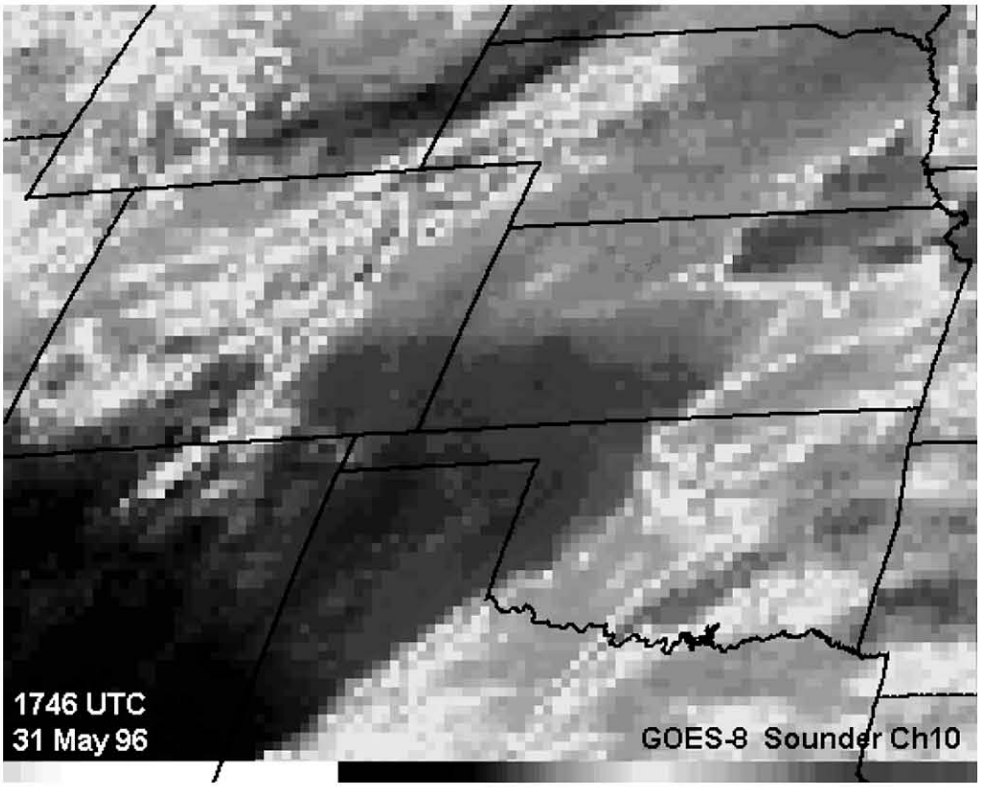

Fig. 17. Image made from GOES-8 sounder channel 10 data (centered at 12.66 μm) taken at 1746 UTC 31 May 1996. This channel responds to lower-level, tropospheric water vapor and peaks around 675 mb. It has a strong response between 850 and 500 mb. Notice that the area in northwest Kansas is slightly cooler (more moist) than the area in southwest Kansas.

Several important storm-scale features can be seen on the GOES imagery as the storms in the LTO-generated line reach maturity. For example, consider the series of GOES-8 visible images in Fig. 18. The image

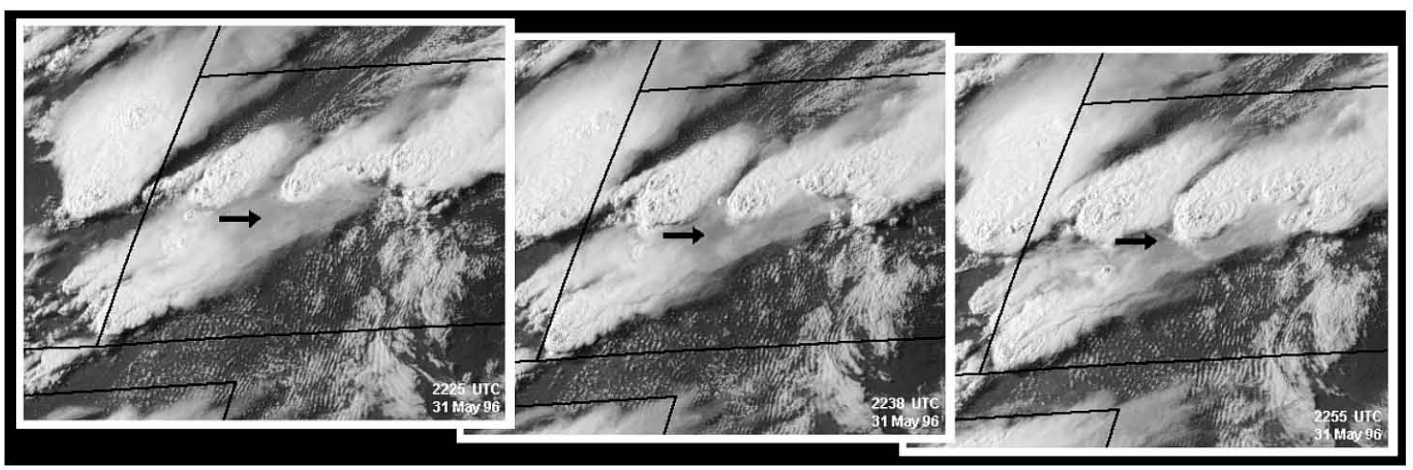

Fig. 18. Time series of GOES-8 visible images from 31 May 1996. Times as labeled. The sequence illustrates the dissipation of cirrus cloudiness as it approaches the Ness City storm in Kansas. As the cirrus dissipates, the flank of the Ness City storm becomes visible.

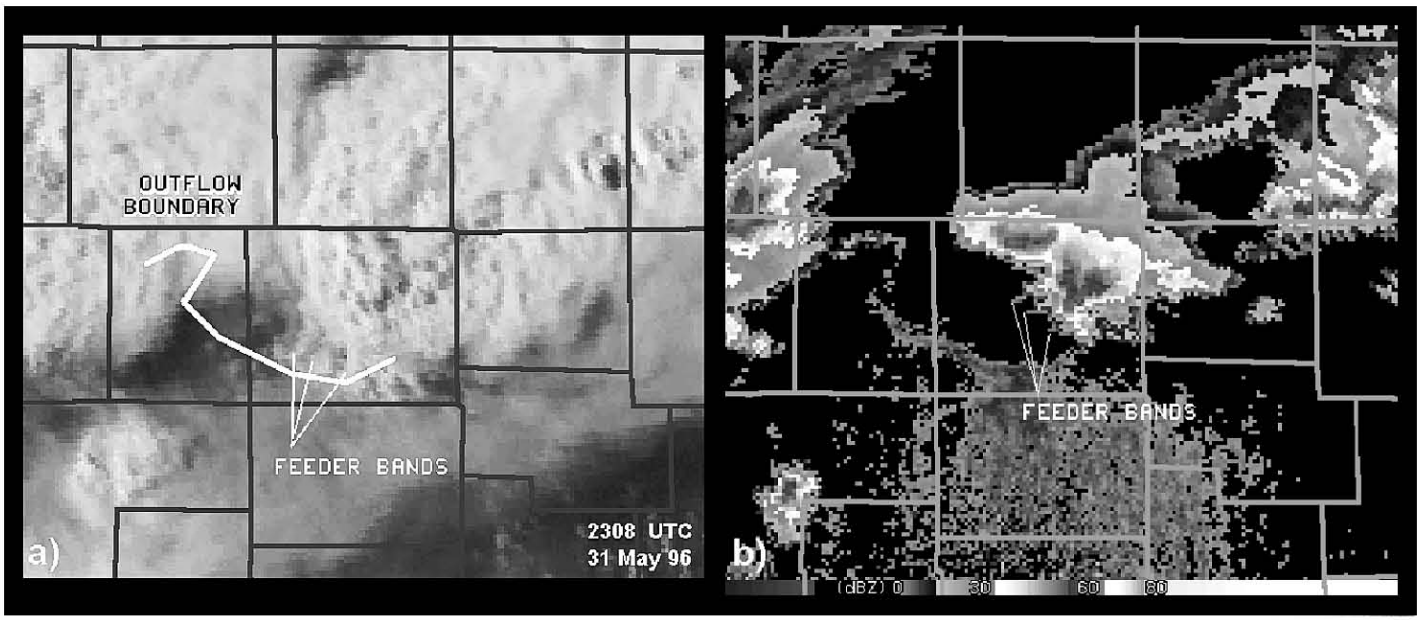

Fig. 19. a) Visible satellite image re-mapped to radar projection at 2308 UTC 31 May 1996. Multiple "feeder bands" are as indicated. White outflow boundary position is from radar. b) Dodge City, Kansas, WSR-88D reflectivity product valid 2308 UTC 31 May 1996 with 0.5° elevation scan shown and features of interest as indicated.

sequence shows anvil cirrus from the convection in extreme southwest Kansas *thinning* appreciably as it approaches the center storm in the line. The LTO storm in question produced an F2 tornado, which touched down at 2306 UTC near the town of Ness City, Kansas. Due to the intensity of the tornadic activity, and the observed cirrus thinning, we believe that the Ness City storm was better organized than the one in southeast Colorado. The thinning cirrus may have been the result of anvil-level subsidence associated with a developing high pressure region aloft (similar to that described, for example, by Schmidt and Cotton 1990). Furthermore, WSR-88D data (not shown) indicate that the circulation in the Ness City storm was better organized and more intense. Regardless of the mechanism causing the phenomenon, the thinning allows us to view the lower part of the storm where multiple flanks can be seen on the southern side of the cell. The development of multiple flanks is known to be an indicator of severity in mature thunderstorms (e.g., Weaver and Purdom 1995, Browning et al. 1997). In this case, the flanking feature appeared well before tornado touchdown. Figure 19 shows a comparison of the visible satellite imagery with radar reflectivity. Notice that the two data sets complement one another. For example, the multiple "feeder bands" show up rather well on satellite imagery (Figs. 19a, 18c, or 13), while the newly-generated, storm-scale LTO boundary associated with this cell is nearly entirely obscured by cirrus. The radar reflectivity (Fig. 19b), however, shows this feature nicely.

Quantitative infrared cloud-top temperature trends and subjective severe weather signatures (such as the enhanced-V, McCann 1983) can also provide clues to storm morphology, and provide a means for anticipating short-term storm behavior. For example, the Ness City storm exhibited a cloud top temperature trend, which appears to have coincided with the tornadic activity described in the local storm reports, storm data, and the available video. Figure 20 shows the 10.7 μm cloud-top temperatures from GOES-8 for the period 2255 - 2339 UTC. Notice that the coldest top reaches a minimum temperature of -71.1C by 2259 UTC. The cloud top cooling culminates in the appearance of an enhanced-V signature (Fig. 21) which results from significant upward motion and ejection of mass by the overshooting top into the stratosphere. Following this evolution, significant cloud top warming takes place (5.2 °C warming in 5 minute), followed by the touch down of an F0, then an F2, tornado. In fact, at 2309 UTC, the cold cloud top (overshooting top on visible imagery) was situated close to Ness City where the tornado was occurring. WSR-88D volume scans can be combined with satellite imagery to establish such relationships — even in an operational environment. Contemporaneous WSR-88D radar imagery revealed the presence of a classical supercell echo with high reflectivity, mesocyclone and tornadic signatures through a deep layer. Comparison of the IR and visible data for the Ness City storm do show pronounced overshooting tops and a warm wake associated with the extremely long cirrus plumes — another sign of intense, long-lived convection.

6. Concluding Remarks

This paper illustrates a number of uses for the new generation GOES data. Topics discussed include the identification, tracking and extrapolation of baroclinic lifting zones associated with short-wave troughs, nighttime identification of LTO boundaries using the fog/stratus product, identification of stratiform cloud decks associated with the LLJ using this same product, detecting a surface circulation via tracing cumu-

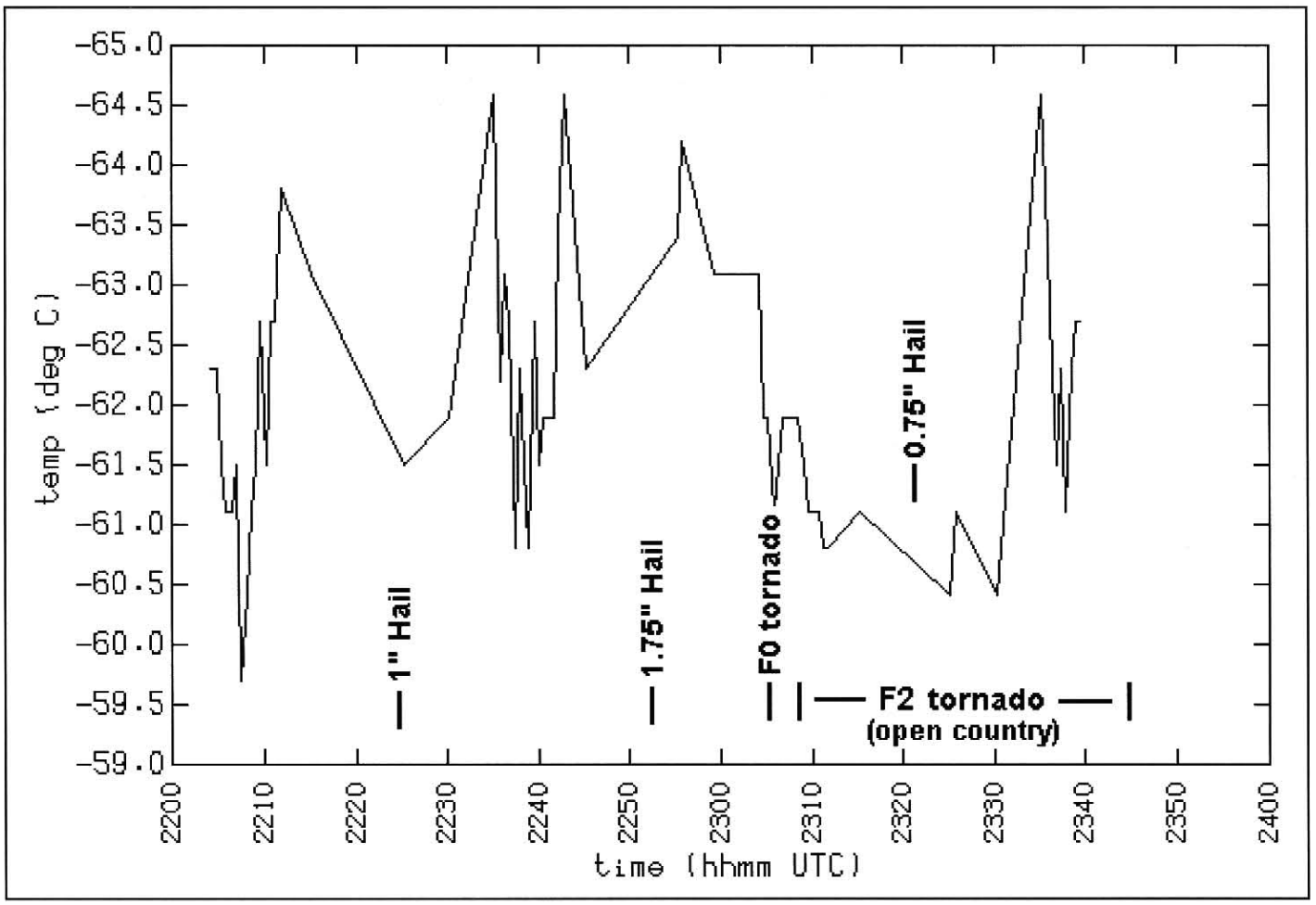

Fig. 20. Plot of the coldest GOES-8, 10.7 μm cloud top temperatures as a function of time for the Ness City, Kansas storm of 31 May 1996. Data intervals range from 15-minute to 30-second. Severe events associated with the storm are superimposed.

lus clouds in the visible imagery, using satellite imagery to refine the location of synoptic features such as the warm front, mesoscale boundary layer analysis, analysis of storm scale features and interactions, and many others. An example was presented illustrating how radar data can augment satellite analysis (specifically, internal storm characteristics), and conversely how satellite data can help interpret and even anticipate what is being tracked on radar (e.g., satellite's ability to view the mesoscale region within which the storm is forming and evolving).

The case presented in this paper is now being used as part of the "Nowcasting Convection and Severe Weather" segment of the SatMet (Satellite Meteorology) class at the Cooperative program for Operational Meteorology Education and Training (COMET) in Boulder, Colorado[4]. COMET is one of three primary training centers utilized

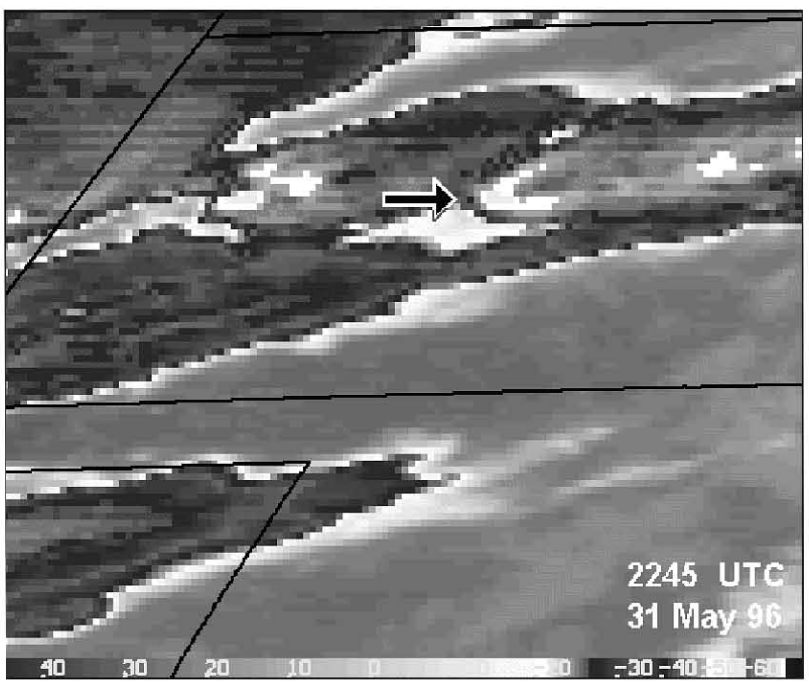

Fig. 21. GOES-8, 10.7 μm image valid 2245 UTC 31 May 1996. Image is centered on Kansas and northern Oklahoma. Arrow indicates enhanced-V feature referred to in text.

[4]The reader interested in learning more about COMET can access their web site at http://www.comet.ucar.edu.

by the National Weather Service. A portion of this material is also used as the basis for a teletraining module offered through the Virtual Institute for Satellite Integration Training (VISIT) program[5].

It is important to realize that neither satellite nor radar is the "end-all and be-all" of remote sensors. Both have their strengths and weaknesses. Even in a nowcasting/warning environment, both sensors can enhance the process. The fact that satellite data is not routinely used in conjunction with radar to formulate severe storm and tornado warnings at the present time is simply because: 1) high-resolution, timely satellite imagery has not been available to NWS forecasters until recently, and 2) there is a general lack of training in this specific application. Now that AWIPS is finally coming on-line in NWS forecast offices across the country, it behooves the forecaster to learn to use satellite imagery with the same degree of expertise demonstrated with the WSR-88D data.

This paper has illustrated the use of satellite imagery for identifying low-level boundaries in an environment where most boundaries were important to triggering convection. Another part of the nowcast problem is that there are many circumstances in which obvious boundaries do not produce deep convection. A forecaster needs to be aware of other factors affecting convection, such as the amount of convective inhibition present on a given day. The negative side of this issue might be a "logical next step" in the study of low-level boundaries.

Acknowledgments

The research presented in this study was performed under NOAA Grant #NA67RJ0152. The authors would like to extend their thanks to Al Pietrycha (NCAR/RAP) and Bill Eckrich (Larimer County Sheriff's Office) for allowing us to use their videos of the southeastern Colorado storms, and to Fred "Fritz" Kruse (NWS/DDC) for his footage of the Ness City, Kansas tornadoes.

Authors

John F. Weaver is a NOAA/NESDIS (National Oceanic and Atmospheric Administration)/(National Environmental Satellite, Data, and Information Services) research meteorologist working at the Cooperative Institute for Research in the Atmosphere (CIRA) at Colorado State University in Fort Collins, Colorado. The facility has one of the most robust satellite ground stations in the country, along with a large staff of scientists skilled in satellite data analysis. Mr. Weaver specializes in developing new techniques for nowcasting and forecasting severe weather including tornadoes, hailstorms, flash floods and severe downslope winds. He earned a B.S. in Mathematics at Colorado State University in 1968, and an M.S. in Atmospheric Science from the University of Wyoming in 1975.

John F. Dostalek holds a research associate position at CIRA. His interests include using both geostationary and polar-orbiting satellite data to investigate the nature of severe thunderstorms and mid-latitude cyclones. He received a B.S. in Physics from The Pennsylvania State University in 1993 and an M.S. in Atmospheric Science from the University of Wisconsin-Madison in 1995.

Brian C. Motta is a research meteorologist at CIRA. Mr. Motta specializes in satellite and radar remote sensing and develops new techniques and visualizations to improve warning, nowcasting and forecasting services. He has been working in weather forecasting and warning support since 1988 and earned a B.S. in Meteorology at Lyndon State College in 1992. He has taken additional graduate-level courses in Atmospheric Science and Education at the University of Alabama in Huntsville, Alabama and at Colorado State University, in Fort Collins. He has also taken advanced level courses at the Cooperative Program for Operational Meteorology, Education and Training (COMET) facility in Boulder, Colorado.

Dr. James F.W. Purdom is a research meteorologist and Director of the Office of Research Applications, NOAA/NESDIS. Dr. Purdom is a nationally recognized expert in satellite meteorology and has published in books, scientific journals, conference proceedings and on Internet Web sites. His research has focused on mesoscale aspects of severe and tornadic thunderstorm environments. He received the 1996 NWA Special Award for his extraordinary accomplishments significantly contributing to operational meteorology. He earned an A.B. in Mathematics and Physics from Transylvania College in 1965, an M.S. in Atmospheric Science from Saint Louis University in 1968 and a Ph.D. in Atmospheric Science from Colorado State University in 1986.

References

Browning, P., J.F. Weaver, and B. Connell, 1997: The Moberly, Missouri tornado of 4 July 1995. *Wea. Forecasting*, 12 (4), 915-927.

Cutting, J.E., and D.R. Proffitt, 1981: Gait perception as an example of how we may perceive events. *Intersensory Perception and Sensory Integration* (R.D. Wak & H.L. Pic, editors), Plenum Press, New York, 436 pp.

_____ , 1982: The minimum principle and the perception of absolute, common, and relative motions. *Cognitive Psychology*, 14, 211-246.

Dostalek, J.F., J. F. Weaver, J.F.W. Purdom, and K. Y. Winston, 1997: Nighttime detection of thunderstorm outflow using a GOES-9 combined image product. *Wea. Forecasting*, 12, 948-951.

Ellrod, G.P., 1994: Detection and analysis of fog at night using GOES multi spectral infrared imagery. *NOAA Tech. Rep. NESDIS* 75, 22 pp. [Available from Nancy Everson, NOAA/NESDIS/ORA/ARAD, NOAA Science Center Room 601, 4700 Silver Hill Road, Stop 9910, Washington. DC 20233-9910.]

[5]The VISIT web site is at http://www.cira.colostate.edu/ramm/visit/visithome.asp

Fujita, T.T., and A. Pearson, 1976: Results of FPP classification of 1971 and 1972 tornadoes. *Proc. of the Symposium on Tornadoes, Texas Tech University*, Lubbock TX, 142-145.

McCann, D.W., 1983: The enhanced-V, a satellite observable severe storm signature. *Mon. Wea. Rev.*, 111, 887-894.

Menzel, W.P., and J.F.W. Purdom, 1994: Introducing GOES-I: The first of a new generation of geostationary operational environmental satellites. *Bull. Amer. Meteor. Soc.*, 75(5), 757-781.

NOAA, 1996: *Storm data and unusual weather phenomena with late reports and corrections.* 38(5), NESDIS, National Climatic Data Center.

RAMM, 1996: GOES 3.9 μm channel tutorial. [This product is available on-line at: http:/www.cira.colostate.edu/ramm/goes39/cover.htm]

Schaefer, J.T., 1973: The motion and morphology of the dryline. *NOAA Tech Memo ERL NSSL-66*, National Severe Storms Laboratory, Norman, Oklahoma 73069, 81 pp.

Schmidt, J.M., and W.R. Cotton, 1990: Interactions between upper and lower tropospheric gravity waves on squall line structure and maintenance. *J. Atmos. Sci.*, 47, 1205-1222.

Weaver, J.F. and J.F.W. Purdom, 1995: An interesting mesoscale storm-environment interaction observed just prior to changes in severe storm behavior. *Wea. Forecasting*, 10, 449-453.

Wertheimer, M. 1937: Laws of organization in perceptual forms. *A Source Book in Gestalt Psychology*, (W.D. Ellis, editor). Routledge and Kegan Paul, London, 286pp.

Note: Two of the original figures for this manuscript were in color, but the article was published in black and white. This PDF utilizes the color version of these figures.